A New Method for Estimating Age-At-Death From the First Rib

Elizabeth A. DiGangi,[1,2]* Jonathan D. Bethard,[2,3] Erin H. Kimmerle,[4] and Lyle W. Konigsberg[5]

[1]*International Criminal Investigative Training Assistance Program (ICITAP)-Colombia, Bogotá, Colombia*
[2]*Department of Natural and Behavioral Sciences, Pellissippi State Technical Community College, Knoxville, TN 37933*
[3]*Department of Anthropology, The University of Tennessee, Knoxville, TN 37996*
[4]*Department of Anthropology, University of South Florida, Tampa, FL 33620*
[5]*Department of Anthropology, University of Illinois at Urbana-Champaign, Urbana, IL 61801*

KEY WORDS age estimation; forensic anthropology; bioarcheology; transition analysis; paleodemography

ABSTRACT A new method for estimating adult age-at-death from the first rib was developed as a modification of the Kunos et al. (Am J Phys Anthropol 110 (1999) 303–323) method. Data were collected on three aspects of the first rib (costal face, rib head, and tubercle facet) for 470 known-age males of Balkan ancestry collected as evidence during investigations conducted by the International Criminal Tribunal for the former Yugoslavia (ICTY). Ages-at-death range from 12 to 90 years (mean of 47.7 years). Several variables were extracted from the original study utilizing all three skeletal aspects of the first rib. This list was modified to 11 variables as preliminary tests on seriations of the samples were undertaken. A cumulative probit model with age measured on a log scale was used to calculate the mean and standard deviation of the ages-of-transition for each component. Multivariate analysis of the three components was also performed. The lowest correlation ($r = 0.079$, controlling for age) was between the geometric shape of the costal face and the surface texture of the tubercle facet. Assuming a correlation of zero, these two traits were used to calculate the highest posterior density regions for estimating individual ages-at-death. Age-at-death estimates generated from 50 and 95% posterior density regions indicate that this method captures age-related change reaching the ninth decade. The Bayesian statistical approach used here produced a valuable and promising new method for estimating age-at-death. Additional research is necessary to determine if these highest posterior density regions produce results highly correlated with age in other samples and its applicability to females. Am J Phys Anthropol 138:164–176, 2009.

Physical anthropologists are often faced with the problem of developing a biological profile from incomplete human skeletal remains. Recent large scale investigations involving mass graves or mass disasters compound this challenge. Elements commonly used for establishing age-at-death such as the pubic symphysis and the sternal aspect of the fourth rib are sometimes absent, body parts may be commingled, or are frequently damaged. In addition, multiple studies have shown that using a multivariate approach when aging a skeleton is far more accurate than using one method alone (Baccino et al., 1999; Martrille et al., 2007). This reality underscores the importance of developing aging methodologies from a broad range of skeletal elements. As a result, numerous methods for age-at-death estimation have been developed and utilized in physical anthropology. Although some methods utilize the histomorphometric structure of bones and teeth to derive age-at-death estimates, the most commonly utilized techniques rely on an investigator to evaluate macroscopic characteristics of various skeletal structures (see Jackes, 2000 for a review). Moreover, recent statistical advances used for developing age-at-death estimation methods have been reported by numerous researchers (Hoppa and Vaupel, 2002; Igarashi et al., 2005) that reduce bias resulting from the demographic structure of the reference population.

Anthropologists who rely on age-at-death estimates as part of their dataset must first recognize the uniformitarian assumption that allows for such inferences in the first place. The fundamental point is that while aging is a variable process, such variation is constrained in a predictable pattern (Milner et al., 2000). Under this assumption, workers who seek to estimate age-at-death in archeological or forensic skeletal samples should be able to apply osteological standards developed from documented anatomical skeletal collections.

Additional Supporting Information may be found in the online version of this article.

This study does not represent in whole or in part the views of the United Nations but those of the authors.

Grant sponsor: The University of Tennessee (Graduate School Professional Development Award).

*Correspondence to: Elizabeth A. DiGangi, ICITAP-Colombia, Calle 125 #19-89, Bogotá, Colombia. E-mail: edigangi@yahoo.com

Received 2 November 2007; accepted 30 June 2008

DOI 10.1002/ajpa.20916
Published online 18 August 2008 in Wiley InterScience (www.interscience.wiley.com).

Moreover, there is individual variability in rates and degrees of the aging process. As a result of such intrasubject variability, biological age and chronological age are not synonymous (Kemkes-Grottenthaler, 2002). More specifically, chronological age is deduced from variables that are correlated with biological aging (Arking, 1998). Although biological age markers do not necessarily represent chronological age for a variety of reasons, they are nevertheless used to estimate chronological age as biological change occurs on a predictable continuum through time (Kemkes-Grottenthaler, 2002). The rate of this process is influenced by genetic, environmental, and health-related modifiers. In other words, a number of factors influence when individuals reach different biological stages: genetics, sex, and activity patterns, among others, have all been implicated (Hoppa, 2000; Jackes, 2000; Kemkes-Grottenthaler, 2002). As a result, different individuals will reach these biological stages at times that are not necessarily correlated with chronological age (Jackes, 2000; Kemkes-Grottenthaler, 2002). The challenge therefore remains to capture information from the skeleton that is most closely linked to chronological age in order to provide a reliable age range estimate.

Although the precise correlation between skeletal markers and chronological age remains elusive, physical anthropologists have made great strides in improving age estimation techniques since the early days of skeletal biology. Today, anthropologists have demonstrated that the best age-at-death estimates are generated by using a multifactorial approach that utilizes a suite of morphological age indicators (Baccino et al., 1999; Martrille et al., 2007). Jackes (2000) adds that physical anthropologists should no longer utilize common aging techniques without recognizing the numerous types of biases associated with them. Such biases include the degree of age-related information contained within specific skeletal traits, as well as sampling strategies and statistical methods used to develop age estimation methods (Jackes, 2000).

Another difficulty associated with adult age-at-death estimation concerns estimating age-at-death for skeletons of older-aged individuals. Traditional methodologies typically lump adults over the ages of 50–60 years in an open-ended cohort, 50+ years age category (Milner et al., 2000). Consequently, this produces a shortcoming that impacts anthropological interpretations of life expectancy by implying that archeological populations did not have a life expectancy past 50 years. Both Jackes (2000) and Milner (personal communication, 2005) contend that it is unwise and unrealistic to assume that individuals in archeological populations did not live past 50 years of age. These are clear limitations in the usefulness of the biological profile for forensic applications as well.

An additional problem regarding age-at-death estimation involves missing data due to taphonomic processes as outlined by numerous researchers (Buikstra and Cook, 1980; Walker et al., 1988; Jackes, 2000; Milner et al., 2000; Paine and Boldsen, 2002; Wittwer-Backofen and Buba, 2002). Soil characteristics sometimes destroy skeletal tissues, animal activity may result in missing and/or damaged elements, and poor excavation techniques can damage or fail to recover skeletal elements. According to Walker et al. (1988), poor preservation often makes age determinations difficult and sometimes forces workers to use methods that yield inferior results. Specific skeletal structures such as the pubic symphysis, auricular surface, and sternal ends of the ribs are commonly subjected to taphonomic processes and are often not recovered or are too damaged to contribute to an osteological analysis. Additional taphonomic biases result from differential burial practices that can lead to missing or underrepresented sex and age cohorts.

To address the aforementioned concerns, numerous scholars participated in a 3-day workshop conducted by the laboratory of survival and longevity at the Max Planck Institute for Demographic Research in Rostock, Germany in June of 1999. The purpose of the workshop was to provide anthropologists with an identical, known-age dataset to test and assess their statistical techniques (Hoppa and Vaupel, 2002). Although participants were able to test and refine methods, a more fundamental discourse emerged during the workshop. A theoretical framework coined the "Rostock Manifesto" was adopted by all scholars in attendance (Hoppa and Vaupel, 2002). When followed, anthropologists agree that it provides a suitable framework for producing accurate adult age-at-death estimates (Igarashi et al., 2005). Although a key component of the Rostock protocol calls for estimating the entire age-at-death distribution $f(a)$ before estimating the age-at-death of any individual skeleton, Boldsen et al. (2002) assert that target populations must be large enough to generate acceptable estimates of $f(a)$. They argue that many samples in both archaeological and forensic contexts are too small to apply such an approach and present a new method to reconcile this problem.

Boldsen et al. (2002: p 75) presented transition analysis as a method for age-at-death estimation that they believe address the four "analytical difficulties" regarding adult age-at-death estimation. These difficulties include: 1) avoiding the large uncertainty associated with age estimation; 2) age mimicry that results from the age-at-death distribution of the reference sample; 3) effective ways to correlate multiple skeletal indicators of age; and 4) developing methods that code morphological changes as they relate to age. Transition analysis estimates the timing of transition from one aging stage or phase to the next by treating each transition as a distinct event (Boldsen et al., 2002).

The fourth rib aging method (Ïsçan et al., 1984a,b, 1985; Ïsçan and Loth, 1986) has become popular as one strategy for aging a skeleton. Although this method has been utilized successfully by several researchers (Dudar et al., 1993; Russell et al., 1993; Yavuz et al., 1998; Yoder et al., 2001), there are some limitations that Kunos et al. (1999) indicate, including the fact that the fourth rib can be misidentified in unarticulated skeletons or that damage to its sternal aspect can preclude its use as an age indicator. In addition, Kunos et al. (1999) argue that relying solely on the morphological changes of the costal face, as the fourth rib aging method does, is not a complete method for estimating age-at-death because it ignores other aspects of the rib that change throughout life, such as the head and tubercle. As a result, Kunos et al. (1999) devised a method utilizing these three aspects in combination (costal face, rib head, and tubercle facet) for estimating age-at-death from the first rib. They utilized the Hamann-Todd skeletal collection, with the reference sample size of 74 individuals and test sample size of 182 individuals. The first rib was chosen because it is easily identifiable, it is not influenced by mechanical stress in the same manner as the lower ribs, it is more

likely to be preserved intact in forensic and archeological contexts, and it exhibits a prolonged span of remodeling into the eighth decade (Kunos et al., 1999).

Most of the commonly used methods for estimating age-at-death such as the pubic symphysis (Brooks and Suchey, 1990), the auricular surface (Lovejoy et al., 1985; Buckberry and Chamberlain, 2002), and fourth rib (Işçan et al., 1984a,b, 1985; Işçan and Loth, 1986) involve the use of descriptive phases into which a particular skeletal element is categorized. Each of these phases is developed to include its own range of age-at-death parameters. In contrast, Kunos et al. (1999) elected to use a different approach, the target-age approach, whereby the three aspects of the rib under observation (costal face, rib head, and tubercle facet) are evaluated on the basis of specific morphology, and these results generated into a table of morphological changes associated with age (see Kunos et al., 1999: Tables 5–7). Kunos et al. (1999) seriated the degree of morphological changes for the first rib by age, and therefore a target age that best matches the morphology of a particular rib can be determined based on this seriation sequence. Although this approach worked well with Kunos et al.'s target sample drawn from the same population as the reference sample, other researchers have suggested that the method is difficult to apply and does not produce accurate age-at-death estimates (Schmitt and Murail, 2004; Kurki, 2005).

Therefore, using the morphological traits that Kunos et al. (1999) identified, this study offers a new method to estimate age-at-death from the first rib. This method is Rostock-compliant and performs a transition analysis to generate age-at-transitions for age-dependent traits.

MATERIALS

The skeletal material utilized in this study was from presumptively and/or positively identified individuals from single interment graves in Kosovo collected as evidence during the investigation of violations to international humanitarian law conducted by the International Criminal Tribunal for the former Yugoslavia (ICTY)[1]. The data used was from evidence collected during criminal investigations by the ICTY which included demographic and osteological data. This evidence was handled following proper Chain of Custody. The University of Tennessee was given permission to use this data by the ICTY for research on aging. A working relationship was established between The University of Tennessee and the ICTY with the expressed goal of sharing data and results that would aid the Office of The Prosecutor and other agencies working on human identification in the region in their investigations. A vital element of this collaboration was the publication of scientific findings to ensure that any revised biological standards for existing methods or any new method(s) would be admissible in court. This collaboration has resulted in a number of related studies on aging (Berg, 2008; Kimmerle et al., 2008a,b,c; Konigsberg et al., 2008; Prince et al., 2008; Prince and Konigsberg, 2008).

For this study, data were collected on three regions of the first rib (costal face, rib head, and tubercle facet) for 470 known-age males. The ages-at-death for this sample range from 12 to 90 years for males (with a mean of 47.7 years). The current dataset for females was too small for analysis at this time.

METHODS

Method development

As previously discussed, Kunos et al. (1999) employed a seriation technique that while useful in identifying the various morphological changes associated with the aging process, is difficult to apply in practice, when isolated cases are encountered or in situations where there may be a large number of cases but limited time for analysis. As a result, seriated observations from Kunos et al.'s publication were analyzed to identify a number of variables that could be used. The list of morphological changes was collapsed categorically. The method for combining features was based on the following: 1) repetitiveness of observations; 2) clarity of terminology; and 3) presence of traits in the sample under study. The preliminary application of this method resulted in a total of 11 variables: three for the costal face, four for the rib head, and four for the tubercle facet (Table 1). Each region of the rib had different traits associated with it that varied in appearance and had between 3 and 5 ordinal-categorical variants (Tables 2–4). When scoring the ribs using the revised variables, two observers (EAD, JDB) chose one variant for each trait. Although ultimately two variables were isolated as being the most robust age indicators, the interested reader is invited to refer to the supplementary file for this manuscript which includes specific descriptions of each variant for the remaining nine variables, as well as photographs of these variants, available online (refer to web address posted on first page of article).

Statistical methodology

To calculate the ages-of-transition for each component, the log-age cumulative probit model was performed. This model is used to determine if the traits coded for are age-dependent by calculating the mean estimated age-at-transition between each observation within the variables. (For example, for the variable "Tubercle Facet: Surface Texture," the model calculated the average transition age between Stage 1: surface is dense and smooth and Stage 2: surface is depressed and irregular). Ages-at-transition is also known as transition analysis, a

[1]"Presumptive" identification does not necessarily mean that the data are unreliable. Typically most identifications are presumptive in situations where large-scale human rights abuses and/or armed conflict has occurred, since whole villages or cities have been destroyed, and as a result not only are the survivors (if any) displaced, but any antemortem records have probably been lost as well. In these cases, a combination of several lines of evidence are used to identify individuals, including the biological profile, investigative evidence (i.e., eyewitness accounts), and the recognition of biological and other traits, such as teeth, clothing, and personal effects. Such "presumptive" identifications have resulted in the repatriation of individuals to their families or communities for burial as well as in the issuance of death certificates. Data used in this study from Kosovo came from early identifications in 2000 which occurred immediately following the conflict there (refer to Kimmerle et al., 2008a). Furthermore, DNA tests conducted on ~100 presumptively identified individuals from Kosovo resulted in positive matches. This further supports the U.N. protocol methodology for the identification of unknown decedents (Kimmerle et al., 2008a).

TABLE 1. Morphological components of first rib[a]

Costal face	Rib head	Tubercle facet
Geometric shape (CF1)	Surface shape (RH1)	Geometric shape of tubercle and neck (TF1)
Surface topography and texture (CF2)	Surface topography (RH2)	Surface topography (TF2)
Margins of face (CF3)	Surface texture (RH3)	Surface texture (TF3)
	Edges of margins (RH4)	Articular margins (TF4)

[a] Adapted from Kunos et al. (1999).

TABLE 2. Revised scoring system for costal face

Trait and score	Description
Geometric shape (CF1)	
1	Narrow, oval, flat surface, and shallow with ridges (line of fusion still evident)
2	Narrow, U-shaped, oval, slightly concave, no ridges on bottom surface
3	Circular and/or wider U-shape, concave
4	Irregular shape, hollowed shell
5	Cortical cavity filled in with bony growth; irregular shape
Surface topography and texture (CF2)	
1	Knobby ridges/billows, irregular
2	Surface smooth, no ridges
3	Microporosity evident
4	Concave
5	Macroporosity
Margins of face (CF3)	
1	Margins rounded/uneven; margins project with scalloped edges
2	Margins irregular, rugged, knobby projections
3	Large spicule(s) along ¼–½ surface of the rim
4	Ossification of spicules along >½ surface rim, thinning osteoporotic bone

TABLE 3. Revised scoring system for rib head

Trait and score	Description
Surface shape (RH1)	
1	Epiphysis unfused; epiphysis fused, shape is flat and circular
2	Shape is oval
3	Shape is irregular
Surface topography (RH2)	
1	Surface is flat or convex
2	Surface is irregular
3	Medio-lateral groove present on superior margin
4	Surface is secondarily flat
Surface texture (RH3)	
1	Dense and smooth
2	Surface depressed and irregular
3	Microporosity present
4	Lipping along margins; macroporosity
Edges of margins (RH4)	
1	Round and smooth; dorsal outer margin continuous with rib neck
2	Rim not well defined, irregular
3	Rim well defined, irregular, sharply angled
4	Exotoses and lipping present

method that allows deductions to be made regarding the transition timing from one stage to the next (Boldsen et al., 2002). By treating each transition as a distinct event, this model can evaluate whether each component of the scoring system is age informative. Statistical models were run in the statistical program "R" (http://www.r-project.org), and the ages-at-transition were calculated using the R function "polr" (with a probit link) in the library "MASS." All of the R scripts and data are made available as an R workspace located online at: https://netfiles.uiuc.edu/lylek/www/ribs.RData. In the following, we refer to specific scripts that can be run to do the analyses.

The cumulative probit allows one to find the probability that an individual who is a particular age would be in a particular rib stage. The simplest example here is from the variable "Rib Head: Surface Shape," as that variable has only three ordered stages. The results section shows that the common standard deviation for the two transitions (from Stage 1 to 2 and from Stage 2 to 3) is 0.5898 on a log scale for age. The two mean ages-to-transition on the log scale are 3.0006 and 3.5314 (see the R script "trans.anal" and run as "trans.anal(4)" for the fourth trait). From these parameters, one can find the probability that an individual who is, for example, age 34.34 years old is in the first stage as one (1) minus the lower tail area (up to 34.34) from a log normal distribution with a mean and standard deviation of 3.0006 and 0.5898. This probability is equal to 0.1819. The probability that such an individual would be in the second stage is the difference between the lower tail areas of log normal distributions with means of 3.0006 and 3.5314 and a common standard deviation of 0.5898. This probability is 0.3148. Finally, the probability that such an individual is in the third stage is the lower tail area from a log normal distribution with a mean of 3.5314 and a standard deviation of 0.5898. This final probability is 0.5033, and the sum of the probabilities (0.1819 + 0.3148 + 0.5033) is equal to one (1) as someone who is 34.34 years old must be in one of the three defined stages (see the R script "toy" for these calculations).

One immediate potential problem with transition analysis is that it assumes some distributional form for the ages-at-transition between stages before estimating the parameters of that distribution (for a two stage system) or distributions (for a three or more stage system). As the ages-at-transition are not themselves observed (only the ages-at-death are observed), there is no direct way to test whether these ages fit the assumed distribution. Mueller et al. (2002) have suggested a kernel density method that allows one to visually check for deviations from the assumed distribution(s), whereas Bera et al. (1984) have described a Lagrange multiplier test to formally test whether the underlying distribution is normally distributed in a probit analysis. This test has been extended to the cumulative probit case by three authors

TABLE 4. Revised scoring system for tubercle facet

Trait and Score	Description
Geometric shape of tubercle and neck (TF1)	
1	Unfused; fused with flat, oval shape; cresting of neck with defined ridges
2	Teardrop shape with pointed medial margin
3	Oval, crescent shape, swollen superior edge
4	Irregular and/or circular profile that projects
Surface topography (TF2)	
1	Rounded/bulbous
2	Flat
3	Concave
4	Irregular; macroporosity
Surface texture (TF3)	
1	Dense and smooth
2	Surface depressed and irregular
3	Microporosity present
4	Lipping along margins; extensive porosity and lipping, altering texture
Articular margins (TF4)	
1	Round and smooth
2	Elevated rim
3	Rugged
4	Superior margin depressed; increase in rugosity; prominent osteophytes and/or lipping

TABLE 5. Lagrange multiplier chi-square tests of normality

Trait	Normal χ^2	*P*-value	Log-normal χ^2	*P*-value
CF1	61.57	<0.0001	66.61	<0.0001
CF2	1.75	0.4169	3.18	0.2044
CF3	15.57	0.0004	24.42	<0.0001
RH1	1.99	0.3692	2.65	0.2658
RH2	4.02	0.134	4.79	0.0913
RH3	10.82	0.0045	18.83	0.0001
RH4	0.13	0.9376	0.04	0.9798
TF1	9.35	0.0093	8	0.0183
TF2	1.67	0.4349	2.05	0.3582
TF3	3.22	0.1998	5.27	0.0717
TF4	0.9	0.6369	0.54	0.7625

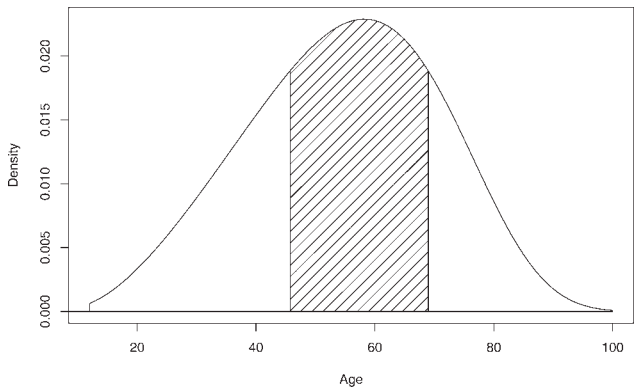

Fig. 1. Posterior density of age conditional on the Makeham model and being in Stage 3 of Rib Head: Surface Shape.

(Johnson, 1996; Glewwe, 1997; Weiss, 1997). These extensions are equivalent and we have programmed the test (following Johnson's presentation most closely) in R. Running the R script "LM.ribs" on the fourth trait (LM.ribs(4)) produces a chi-square statistic with two degrees of freedom equal to 2.6500, which gives a probability value of 0.2658. See Table 5. This demonstrates that there is no detectable departure from a log normal distribution (the default distribution in our script) for ages-at-transition of the variable "Rib Head: Surface Shape." A similar test can be run as "LM.ribs(4,F)" which tests for normality.

Bayes' theorem can be used to invert the problem to one of age estimation, rather than finding the probability that someone of a known age would be in a particular rib stage. In this context, Bayes' theorem is:

$$f(a|i) = \frac{f(a|\theta)\Pr(i|a)}{\int f(a|\theta)\Pr(i|a)da}$$

where $\Pr(i\,|\,a)$ is the probability that someone at exact age "a" is in the observed rib stage i. This probability comes from the transition analysis, as shown previously. The probability density function $f(a|\theta)$ is the prior probability of death at exact age "a" given the parameters (θ) in a hazard model. The denominator gives the integral of the product of these two probabilities across age. As an example, in the following analysis a Makeham mortality model will be fit to the 470 individuals in the reference sample. The three estimated parameters are $a_2 = 0.0059$, $a_3 = 0.0045$, and $b_3 = 0.0522$, where "age zero" is at age 12 and the symbols for the parameters follow the Siler five-parameter model (see the R script "Makeham" for estimation and "plot.rib" for a comparison of the 95% confidence intervals on survivorship from the Makeham as versus Kaplan-Meier survivorship). Applying the transition analysis parameters from the previous paragraph and the Makeham model parameters, the highest density for age given that an individual is in Stage 3 for surface shape of the rib head occurs at 58.23 years. Figure 1 shows the complete posterior density of age which has been "normalized" so that it integrates to 1.0. The shaded area represents the 50% highest posterior density (HPD) region, which runs from ages 45.71 to 68.98 years (see the R script "lrage. viewer").

Although examining each of the 11 rib variables individually was a useful first step, it was necessary to consider these variables jointly. This was a difficult analysis because the intercorrelations among rib variables must be considered after "removing" the effect of age. This was done here by considering all pairs of variables, estimating the cumulative probit for each member of the pair, and then estimating each polychoric correlation with the marginal parameters fixed for the individual traits (see the script "fit2.ribs" to estimate the correlation between any pair of traits and "run.corr" to get the correlation matrix). On the basis of the estimated 11×11 polychoric correlation matrix, we identified two variables with the lowest correlation (the costal face geometric shape and tubercle facet surface texture, $r = 0.079$), assumed the correlation is zero, and then used these to present a table of posterior densities of age.

RESULTS

Table 6 gives the common standard deviations and mean ages-to-transition for age on the logarithmic scale for each of the 11 rib traits. These can be used to recover the mode, median, and average age-to-transition on the original scale. Because the log-normal distribution is asymmetric the mode, median, and average are not equal when converted to the original scale. The mode is equal to $\exp(\mu)/\exp(\sigma^2)$, the median is $\exp(\mu)$, and the mean is $\exp(\mu) \times \exp(\sigma^2/2)$. For example, the mode for the first transition of the rib head surface shape is 14.1928 years [$=\exp(3.0006)/\exp(0.5898^2)$], the median is 20.0976 years [$=\exp(3.0006)$], and the mean is 23.9156 years [$= \exp(3.0006) \times \exp(0.5898^2/2)$].

The information provided in Table 6 can also be combined with an informative prior for age-at-death in order to derive HPD regions (as in Fig. 1). To combine such information across more than one trait the correlations between traits (after "removing" the effect of age) must be calculated. Table 7 contains the matrix of these polychoric correlations as well as the sample sizes used to calculate the correlations. Sample sizes for pairs of traits were less than the 470 total individuals due to missing data, ranging from 400 individuals available for the CF2 and RH4 bivariate analysis to 463 individuals for the CF1 and CF3 analysis. As all of the scorings were done as age progressions, all of the correlations are positive. Many of the correlations are substantial with the highest at $r = 0.75$ between CF1 and CF2. The lowest correlation is 0.079 between CF1 (geometric shape of costal face) and TF3 (surface texture of tubercle facet). The standard error for this correlation in the full model estimating marginal effects is 0.0585, giving a z-score of 0.7405 ($P = 0.459$ on a two-tailed test). This is a somewhat time consuming analysis to run, so the results of running the R script "fullfit" are stored in the R object CF1TF3 and the standard error for the correlation can be obtained using: sqrt (solve(−CF1TF3$hess)[10,10]). As the correlation is not significantly different from zero, it can be considered as equaling zero, and the likelihoods from each trait can be multiplied and combined with the prior age distribution to find posterior age distributions. Table 8 gives the 50th and 95th percent highest posterior densities across these two traits (see the script "lrage2" for these calculations). When applied back to the 449 individuals with scores on both traits, the 95% HPD contains 417 individuals (92.87%), whereas the 50% HPD contains 224 individuals (49.89%). These actual percentages (from the script "check.it") are very close to the nominal levels (95 and 50%, respectively). It is not possible to directly expand this method for age estimation beyond two traits because of the rising correlations between traits. This situation also contributes to the utility of the method's application; as there are only two traits involved, the ease of actual application is considerable.

TABLE 6. Standard deviation and mean ages-to-transition (on logarithmic scale) for the eleven ordinal-scored rib traits

Trait	N	St. Dev.	1|2	2|3	3|4	4|5
CF1	463	0.6486	2.6975	3.0690	3.4309	4.1953
CF2	439	0.5619	2.7966	2.8922	3.2701	3.4472
CF3	466	0.4852	3.1349	3.5332	3.8444	
RH1	428	0.5898	3.0006	3.5314		
RH2	428	0.7563	3.0091	3.8668	4.2168	
RH3	428	0.7568	2.8623	3.2721	3.7092	
RH4	427	0.7155	2.9988	3.6543	4.2389	
TF1	457	0.8265	3.0067	3.5420	4.2416	
TF2	456	0.8443	2.7099	3.0578	3.4877	
TF3	456	0.7365	3.1887	3.6960	4.0691	
TF4	457	0.6208	2.8915	3.5133	4.1554	

Application of first rib aging method

The preceding analysis demonstrates that two morphological markers contain age-dependent information. There are only two morphological states that are scored categorically, making the method straightforward in its application. Researchers need only to familiarize themselves with the utilized terminology and morphology (Appendix A) to apply the method correctly. The features used are costal face: geometric shape and tubercle facet: surface texture. Application of the method involves referring to the tables and scoring system presented in the Appendix, and applying those as indicated. Once the scores are obtained for each feature, use the posterior densities presented in Table 8 to obtain the age estimate. For example, perusal of Table 8 reveals that a score of "3" for the costal face and a score of "2" for the tubercle facet has a best point of 32.07 years old at death with a range of 23.1 to 43.9 years old at death in the 50% HPD region. Table 8 presents posterior density regions for all possible combinations of scores, and the combinations of these scores produce age-at-death estimations that include best age estimates reaching the seventh decade,

TABLE 7. Correlations among the eleven ordinal-scored rib traits

	CF1	CF2	CF3	RH1	RH2	RH3	RH4	TF1	TF2	TF3	TF4
CF1	–	0.750	0.471	0.230	0.218	0.174	0.250	0.304	0.195	0.079	0.185
CF2	438	–	0.679	0.362	0.372	0.348	0.381	0.498	0.319	0.373	0.431
CF3	463	439	–	0.163	0.270	0.228	0.281	0.336	0.321	0.220	0.233
RH1	422	401	425	–	0.494	0.485	0.484	0.356	0.251	0.149	0.250
RH2	422	401	425	428	–	0.702	0.617	0.414	0.302	0.252	0.374
RH3	422	401	425	428	428	–	0.711	0.291	0.275	0.260	0.317
RH4	421	400	424	427	427	427	–	0.396	0.296	0.140	0.291
TF1	450	426	453	421	421	421	420	–	0.495	0.426	0.461
TF2	449	425	452	421	421	421	420	456	–	0.572	0.589
TF3	449	425	452	421	421	421	420	456	456	–	0.747
TF4	450	426	453	421	421	421	420	457	456	456	–

The values above the diagonal are polychoric correlations. The values below the diagonal are the sample sizes available for each pair of traits.

TABLE 8. Posterior densities for age given CF1 (costal face geometric shape) and TF3 (tubercle facet surface texture) scores and the Makeham model specified in the text

CF1	TF3	Lower 95%	Lower 50%	Best Point	Upper 50%	Upper 95%
1	1	[12]	[12]	[12]	18.24	39.51
2	1	[12]	[12]	15.10	23.40	50.58
3	1	[12]	13.72	20.19	29.65	57.71
4	1	[12]	21.27	30.46	42.79	66.73
5	1	19.73	37.74	49.45	60.82	79.20
1	2	[12]	[12]	16.34	24.28	51.86
2	2	[12]	17.78	25.26	35.93	61.21
3	2	12.90	23.10	32.07	43.90	67.29
4	2	17.89	33.11	43.95	55.59	75.76
5	2	26.96	46.27	57.26	67.44	83.56
1	3	[12]	14.58	21.29	31.02	58.32
2	3	12.74	22.74	31.59	43.35	66.80
3	3	16.01	29.20	39.34	51.17	72.80
4	3	21.75	39.13	50.23	61.18	79.31
5	3	30.85	50.35	60.87	70.49	85.67
1	4	[12]	21.15	30.31	42.81	67.08
2	4	17.17	32.06	42.98	54.87	75.49
3	4	21.33	38.94	50.26	61.35	79.53
4	4	27.84	47.45	58.39	68.43	84.24
5	4	36.81	56.34	66.19	75.05	88.99

"Best point" is the age with the highest posterior density. "Lower" and "Upper" refer to the bounds for the stated highest posterior density regions. Ages in brackets occur on boundaries.

which surpasses that of most traditional aging methodologies.

DISCUSSION

Utilizing methodological criteria discussed in Kunos et al. (1999), we developed categorical traits for 11 variables of the first rib. Our work, which was based on seriated stages from Kunos et al., was designed to capture age-related stages in a manner quickly and accurately applied. We are optimistic that the two traits we have identified can be used to help estimate age-at-death in unidentified skeletal remains. Although the two traits of costal face: geometric shape and tubercle facet: surface texture were isolated as being the most robust age indicators from a total of 11 analyzed variables, the reader may find more information regarding the other variables in the supplementary file to this manuscript, located online (refer to web address posted on first page of article).

Although we remain optimistic regarding the possible utility of this method, there are several issues that deserve mention. Concerning inter and intraobserver error, the data were not originally collected in such a manner that such error analyses can be done. Besides determining repeatability and reliability of the method, the issue of a possible male bias deserves further exploration in future applications of the method and subsequent analyses. Although posterior density regions are presented here for an exclusively male sample, we are cautiously optimistic that this method can be applied to female cases as well. Our rationale for this in part stems from an example from the commonly cited fourth rib aging method (İşçan et al., 1984a,b, 1985). In that method, the mean age of Phase 7 only deviates by 6.0 years between males and females, which is the widest discrepancy of mean age for all phases between the sexes seen (İşçan et al., 1984a,b, 1985). For this reason, we argue that the first rib method presented here should be extensively tested on other samples to determine if a similar pattern with the first rib emerges.

There is the additional problem that the Lagrange multiplier chi-square tests (see Table 5) indicate that the ages-to-transition are not normally or log-normally distributed for four of the traits (TF1, RH3, CF3, and CF1). One of these traits (CF1) was used in the bivariate analysis because it had the lowest correlation with any other trait. For researchers who see the distributional assumption as problematic, they can use Tables 5 and 7 as the basis for selecting which trait or traits to use in age determination. To our knowledge, this is the first time that the distributional assumption has been formally tested in a transition analysis. As a result, while the fact that about one third of the traits fail to meet the distributional assumptions may be disturbing, we have no basis for comparison to traits from other studies. Further, because we provide Tables 5 and 7, researchers can make their own decisions about which traits to use in an analysis.

A final potential problem with the method as presented here is the assumption of a prior age-at-death distribution. We do not actually see this as a major limitation of the study, because we use an explicit prior. Researchers who wish to use a different prior are welcome to do so.

Overall, the method we have presented here should provide workers with a user-friendly aging methodology. The first rib is unambiguously identifiable, and the costal face and tubercle facet are easily distinguishable from other regions of the bone. Moreover, the categorical scale we developed should be easy for other workers to learn and apply. This method takes criteria discussed in Kunos et al. (1999) a step further than originally published. Rather than referring to a table that lists seriated changes, our work has eliminated those variables that do not provide reliable information about age-related change.

CONCLUSIONS

Depending on the recovered elements, the first rib is shown to provide a robust age-at-death estimate or it may help narrow an estimate when used in combination with other morphological markers. For the 95% HPD region, the combination of scores from CF1 and TF3 present a range of ages that is several decades wide. While this may seem impractical for forensic situations, determining which region to cite when using this method should be a decision that is based upon the level of precision that is needed for a particular analysis and on the availability of other age indicators that can be analyzed. Because there are different stages in the identification process and multiple applications of demographic structures in forensics and bioarcheology, the level of precision is likely to vary in different contexts. As with any age estimation technique, we strongly recommend that researchers utilize this method as part of a multifactorial approach toward estimating age-at-death for any particular set of skeletal remains. When used in tandem with other methods, we suggest that the conditional independence

of the first rib from other features such as the pubic symphysis will contribute to a practical age-at-death estimate.

Part of the utility of this method lies in its equal applicability to younger and older-aged individuals, incorporating adolescence through senescence. The results provide estimates that surpass a lumped elderly adult age category, which is beneficial when aging older adults. Additional research is necessary to determine if these HPD regions produce results highly correlated with age in other samples and the method's applicability to females.

In summary, the method presented here offers numerous advantages. The first rib is a robust skeletal element often recovered even when sternal aspects of other ribs are not. It is easily identifiable and its morphology is unambiguous, even in field contexts. Moreover, the scoring system presented here calls only for the observer to code morphological changes in the shape of the costal face and texture of the tubercle facet, lowering the propensity for intraobserver error.

As with any new aging method, the traits that we have identified as useful age-at-death indicators should be tested on other known-age skeletal samples. As discussed earlier, this method was developed to assist prosecution efforts in the Balkans where human identification and the demographic profiling of victims are essential evidence at trial. It is our hope that this method will have wide applicability in other regions as well; however, only further testing will demonstrate a broader utility.

As biological anthropology develops during the twenty-first century, we must continually work to refine our methodological toolkit. Age-at-death standards developed from seriated sequences of skeletal elements are a good first step in this process; however, analyses must be taken to the next level by utilizing more powerful statistical techniques. Demographic methodologies are now being heavily scrutinized in court, both domestically and internationally. Therefore, we must strive to develop standards that balance statistical robusticity and wide-scale applicability. Until this is accomplished, age-at-death estimation should remain a fundamental avenue of research by biological anthropologists.

ACKNOWLEDGMENTS

We wish to primarily and most importantly acknowledge the victims of the Balkan genocide and their families. It is our hope that this contribution serves to memorialize them, albeit in a small way. We additionally wish to acknowledge and thank Jose Pablo Baraybar for initiating this project. We thank David Tolbert, Peter McCloskey, and Eamonn Smyth of the ICTY Office of the Prosecutor for access and permission to use the data. We also thank Drs. Richard Jantz and Lee Meadows Jantz and the Forensic Anthropology Center at The University of Tennessee. Justin Corle skillfully produced the photographs herein. The Department of Anthropology at The University of Tennessee provided generous support throughout the duration of this project. Permission to use and publish this data was granted by the United Nations, International Criminal Tribunal for the former Yugoslavia, Office of the Prosecutor and Registry.

APPENDIX A

Costal face: Geometric shape

The geometric shape of the costal face is divided into five sequential age-related stages. The shape of the costal face is narrow and oval early in life and becomes irregular later in life. This feature is scored based on the transition from a shape that is narrow with a shallow cortical cavity, to wide and concave, and finally, irregular with a filled-in cortical cavity. Stage 1 consists of a costal face with a narrow and oval shape where the face surface is flat and shallow. Ridges will mark the face surface during this early stage (Figs. A1a,b). In Stage 2, the shape remains narrow and oval, with a developing U-shape. The face surface will be slightly concave, and ridges no longer mark the face surface (Figs. A2a,b). Stage 3 is characterized by a widening U-shape which may also be circular in appearance. Concavity of the face also continues to be present, and it may be marked at this stage (Figs. A3a,b). By the fourth stage, the shape of the face is irregular, and bony growths may be evident. Ossification of the costal cartilage has commenced by this point, and appears as a hollowed shell or cavity in this stage (Figs. A4a,b). By Stage 5, the cortical cavity is filled in with bony growth that may be convex in appearance. The filled-in cortical cavity as well as the shape of the costal face will be irregular (Figs. A5a,b). The scoring system for costal face: geometric shape is given in Table A1.

Tubercle facet: Surface texture

Surface texture of the tubercle facet is divided into four sequential age-related stages. After epiphyseal appearance and later fusion, the texture of the facet is dense and smooth and eventually later in life exhibits extensive macroporosity and lipping along the margins. The first stage is characterized by a tubercle facet that has a convex rounded shape with dense and smooth texture (Figs. A6a,b). In the second stage, the facet is no longer convex, but has a depressed surface that is undulating and may have slight pitting (pockmarks) (Figs. A7a,b). Microporosity characterizes Stage 3 and is defined as pores that penetrate the surface of the bone, with these pores being less than 1 mm in diameter. Pitting, defined as a pockmarked surface of the bone, should not be included in either of the "porosity" categories and instead fits into Stage 2 of depressed and irregular surface texture. Figures A8a,b illustrate microporosity of the tubercle facet. The last stage includes lipping and/or macroporosity (Figs. A9a,b). Macroporosity consists of pores that penetrate the surface of the bone, with the pores larger than 1 mm in diameter. The tubercle facet may show a distinct margin and it is important to distinguish this feature from lipping, defined as an osteophytic growth that extends (slightly or extensively) beyond the margin. It is possible to observe ribs with characteristics of the latter stages with or without traits of the earlier stages; for example, lipping can be present with or without microporosity. In these instances, those ribs are scored as lipped. (This example of scoring in the later (older) stage when earlier (younger) stage features are or are not present is important as this was the proto-

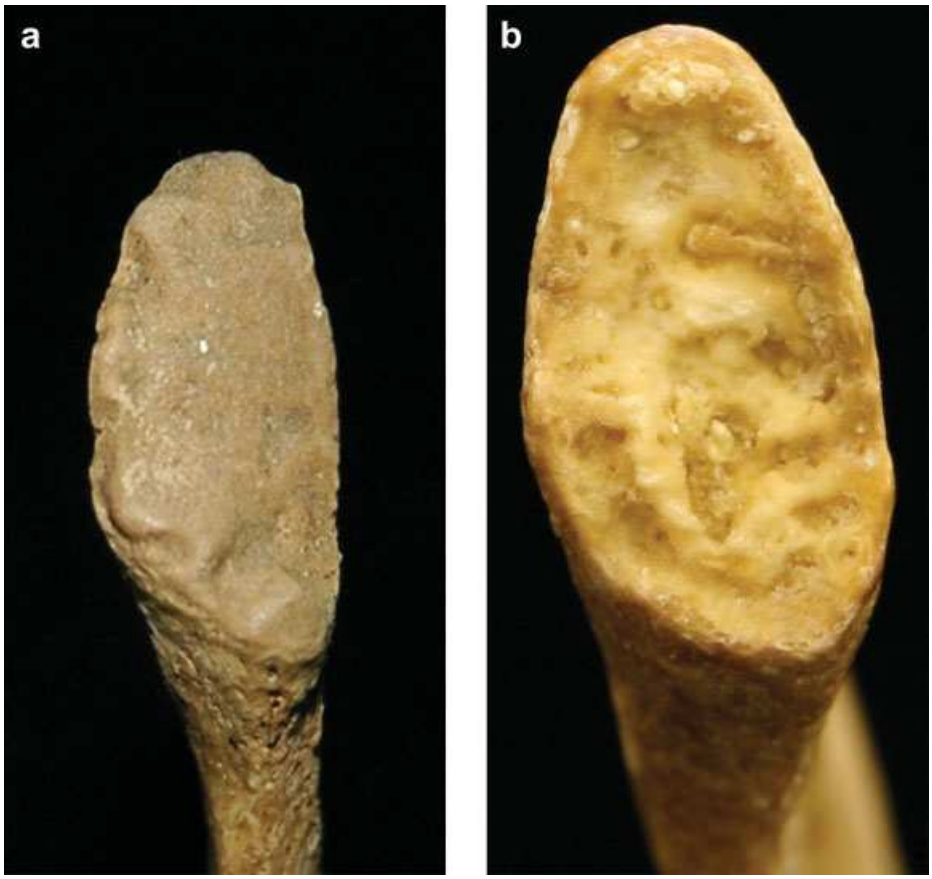

Fig. A1. (**a**) Costal face score no. 1: narrow, oval, shallow with ridges (16-year-old male). (**b**) Costal face score no. 1: narrow, oval, flat surface (25-year-old male). [Color figure can be viewed in the online issue, which is available at www.interscience.wiley.com.]

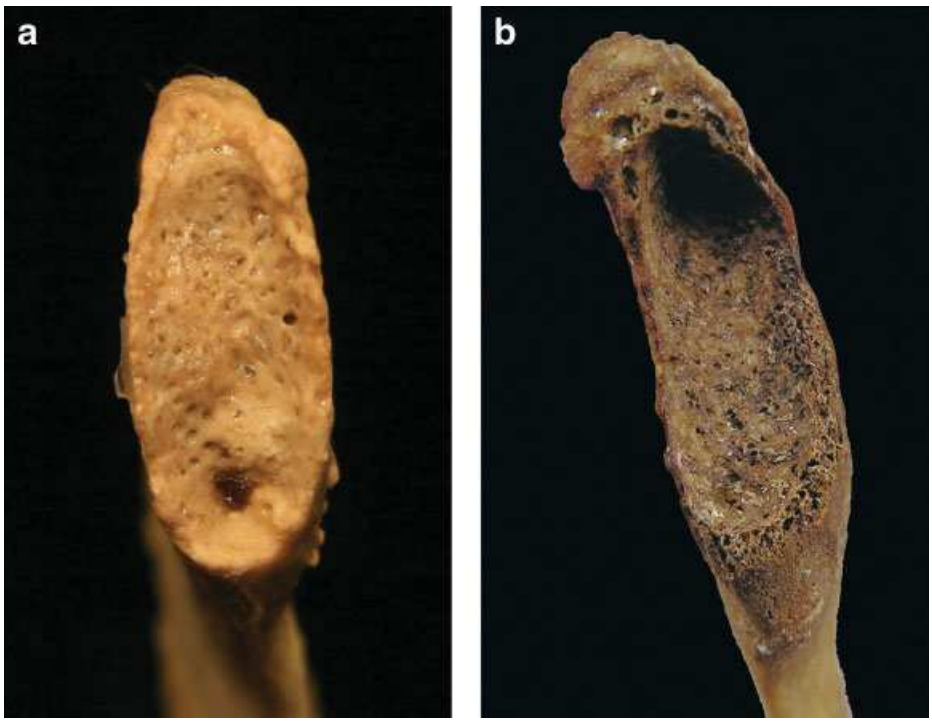

Fig. A2. (**a**) Costal face score no. 2: narrow, oval, concave, no ridges (26-year-old male). (**b**) Costal face score no. 2: narrow, oval, concave, no ridges (41-year-old male). [Color figure can be viewed in the online issue, which is available at www.interscience.wiley.com.]

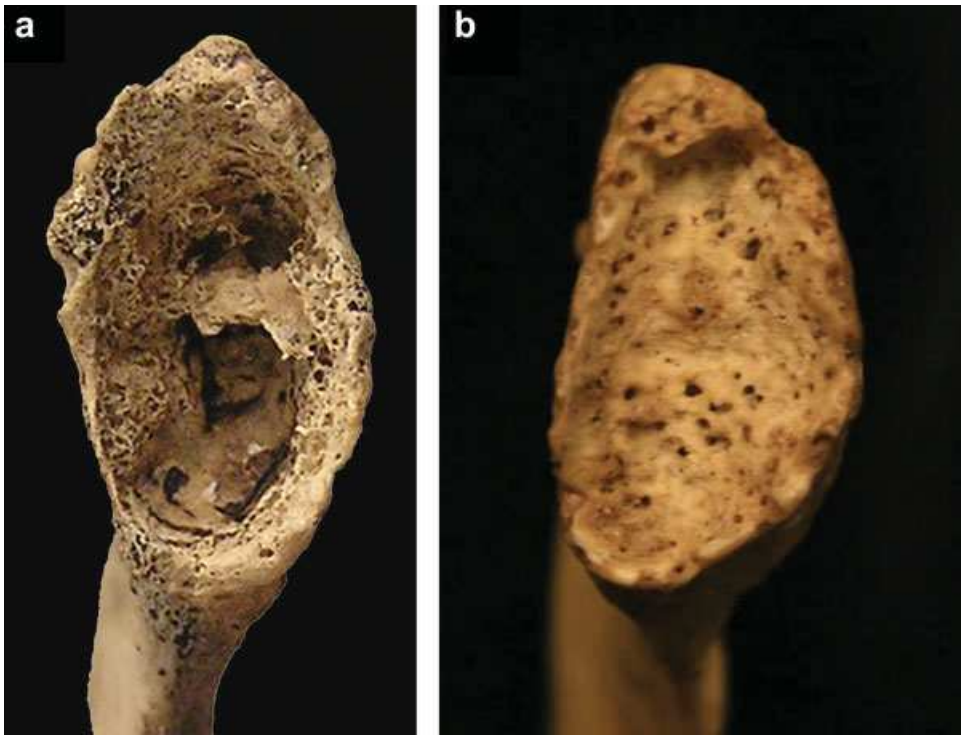

Fig. A3. (**a**) Costal face score no. 3: circular shape, deeply concave (34-year-old male). (**b**) Costal face score no. 3: wide U-shape, deeply concave (34-year-old male). [Color figure can be viewed in the online issue, which is available at www.interscience.wiley.com.]

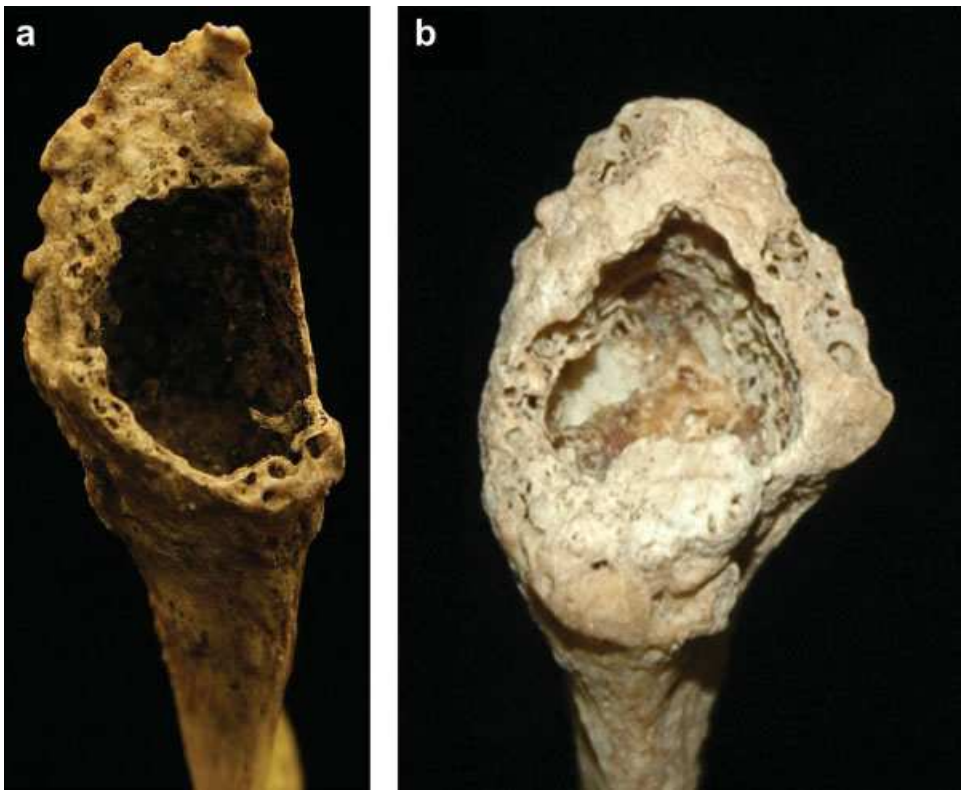

Fig. A4. (**a**) Costal face score no. 4: irregular shape, hollowed shell (54-year-old male). (**b**) Costal face score no. 4: irregular shape, hollowed shell (77-year-old male). [Color figure can be viewed in the online issue, which is available at www.interscience.wiley.com.]

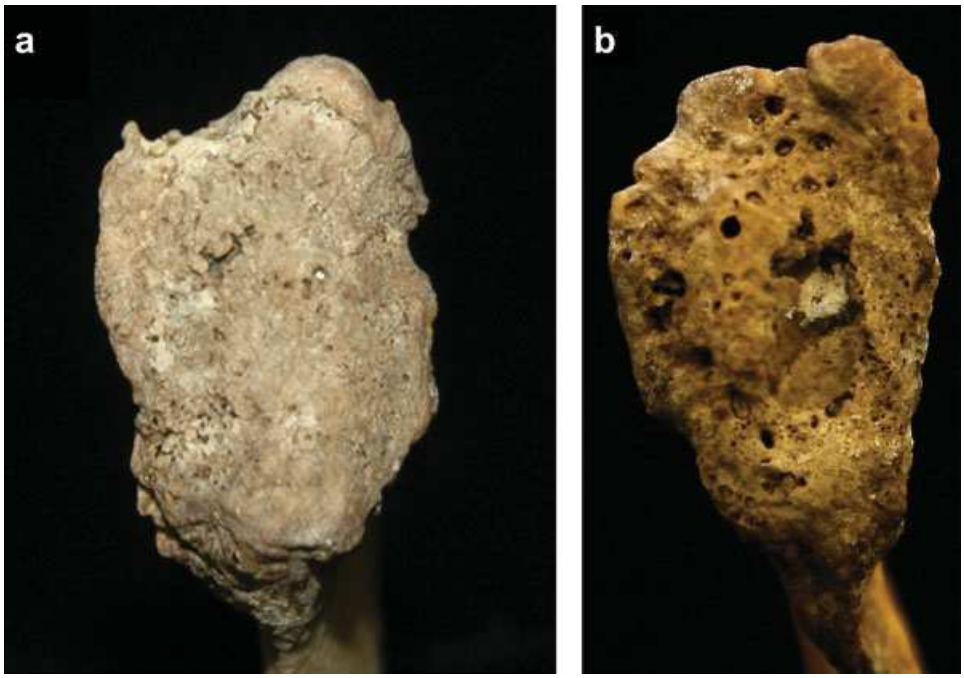

Fig. A5. (**a**) Costal face score no. 5: cortical cavity filled in, irregular (76-year-old male). (**b**) Costal face score no. 5: cortical cavity filled in, irregular (76-year-old male). [Color figure can be viewed in the online issue, which is available at www.interscience.wiley.com.]

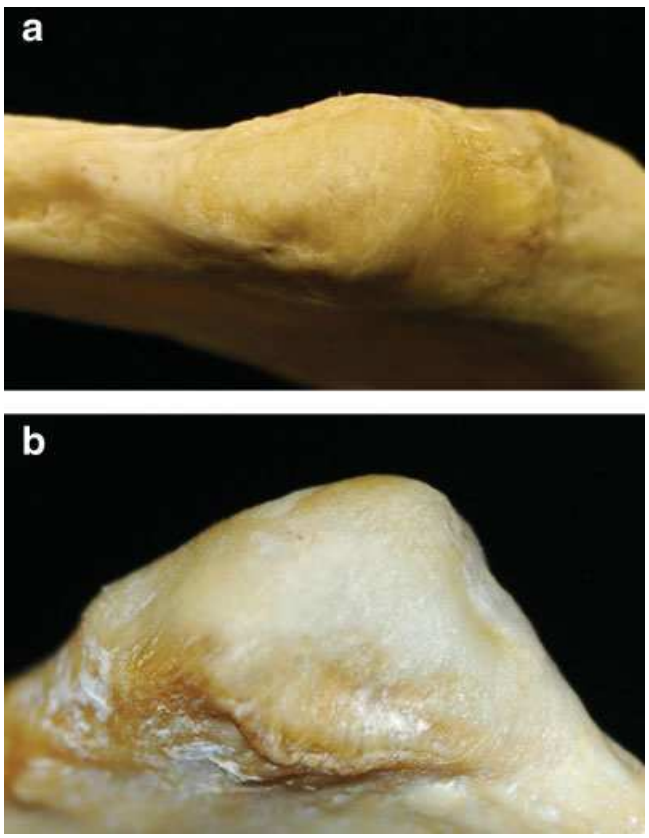

Fig. A6. (**a**) Tubercle facet score no. 1: dense and smooth (27-year-old male). (**b**) Tubercle facet score no. 1: dense and smooth (24-year-old male). [Color figure can be viewed in the online issue, which is available at www.interscience.wiley.com.]

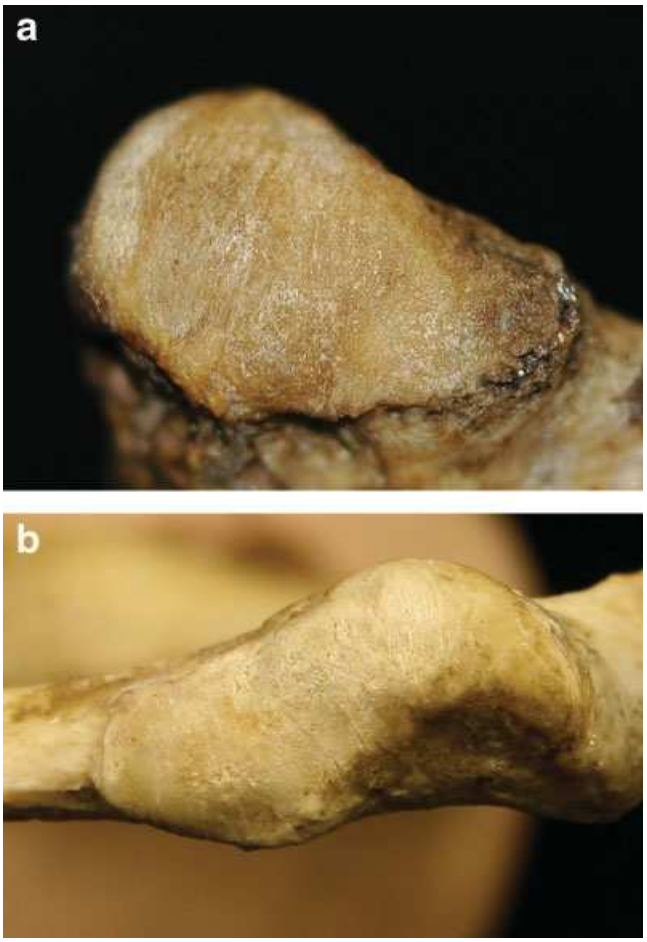

Fig. A7. (**a**) Tubercle facet score no. 2: surface depressed and irregular (61-year-old male). (**b**) Tubercle facet score no. 2: surface depressed and irregular (43-year-old male). [Color figure can be viewed in the online issue, which is available at www.interscience.wiley.com.]

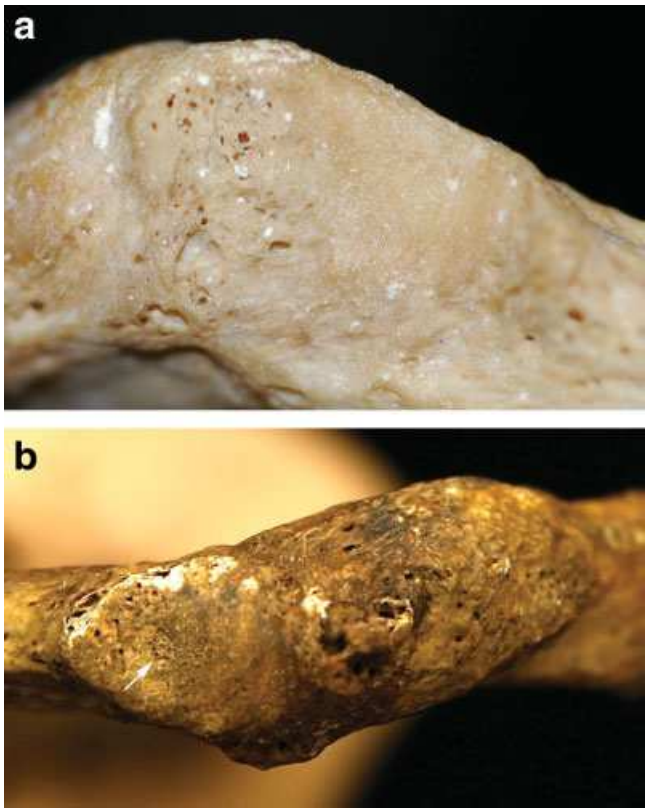

Fig. A8. (**a**) Tubercle facet score no. 3: microporosity (49-year-old male). (**b**) Tubercle facet score no. 3: microporosity (76-year-old-male). Arrow indicates area of microporotic concentration. [Color figure can be viewed in the online issue, which is available at www.interscience.wiley.com.]

col utilized by the initial observers, and therefore the resultant posterior density regions were impacted by this scoring protocol). The scoring system for tubercle facet: surface texture is given in Table A2.

TABLE A1. Scoring system for costal face: geometric shape[a]

Description of geometric shape	Score
Narrow, oval, flat surface, shallow with ridges (line of fusion still evident)	1
Narrow, U-shaped, oval, slightly concave, no ridges on bottom surface	2
Circular and/or wider U-shape, concave	3
Irregular shape, hollowed shell	4
Cortical cavity filled in with bony growth that may be convex; irregular shape	5

[a] see Figures A1a–A5b.

TABLE A2. Scoring system for tubercle facet: surface texture[a]

Description of surface texture	Score
Dense and smooth	1
Surface depressed and irregular	2
Microporosity present	3
Lipping along inferior margin; extensive porosity and lipping, altering texture	4

[a] see Figures A6a–A9b.

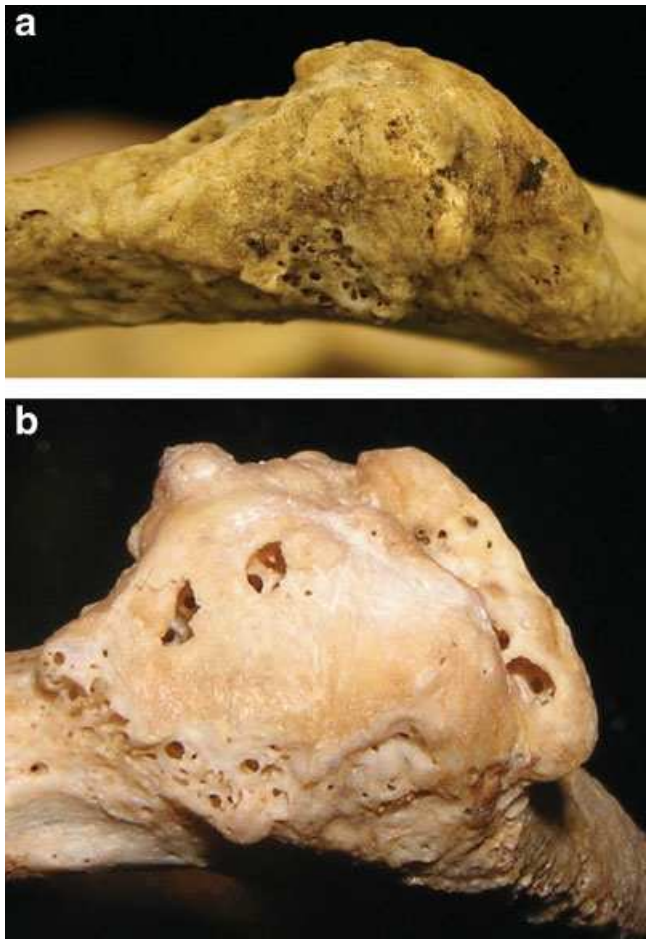

Fig. A9. (**a**) Tubercle facet score no. 4: lipping along margin with porosity (83-year-old male). (**b**) Tubercle facet score no. 4: extensive porosity and lipping (61-year-old male). [Color figure can be viewed in the online issue, which is available at www.interscience.wiley.com.]

LITERATURE CITED

Arking R. 1998. Biology of aging: observations and principles, 2nd ed. Sunderland, MA: Sinauer and Associates.

Baccino E, Ubelaker D, Hayek L, Zerilli A. 1999. Evaluation of seven methods of estimating age at death from mature human skeletal remains. J Forensic Sci 44:931–936.

Bera AK, Jarque CM, Lee LF. 1984. Testing the normality assumption in limited dependent variable models. Int Econ Rev 25:563–578.

Berg GE. 2008. Pubic bone age estimation in adult women. J Forensic Sci 53:569–577.

Boldsen J, Milner G, Konigsberg LW, Wood J. 2002. Transition analysis: a new method for estimating age from skeletons. In: Hoppa R, Vaupel J, editors. Paleodemography: age distributions from skeletal samples. Cambridge: Cambridge University Press. p 73–106.

Brooks J, Suchey J. 1990. Skeletal age determination based on the os pubis: a comparison of the Ascadi-Nemeskeri and Suchey-Brooks methods. Hum Evol 5:227–238.

Buckberry J, Chamberlain A. 2002. Age estimation from the auricular surface of the ilium: a revised method. Am J Phys Anthropol 119:231–239.

Buikstra JE, Cook DC. 1980. Paleopathology: an American account. Ann Rev Anthropol 9:433–470.

Dudar J, Pfeiffer S, Saunders S. 1993. Evaluation of morphological and histological adult skeletal age-at-death estimation techniques using ribs. J Forensic Sci 38:677–685.

Glewwe P. 1997. A test of the normality assumption in ordered probit model. Econ Rev 16:1–19.
Hoppa RD. 2000. Population variation in osteological aging criteria: an example from the pubic symphysis. Am J Phys Anthropol 111:185–191.
Hoppa RD, Vaupel J, editors. 2002. Paleodemography: age distributions from skeletal samples. Cambridge: Cambridge University Press.
Igarashi Y, Uesu K, Wakebe T, Kanazawa E. 2005. New method for estimation of adult skeletal age at death from the morphology of the auricular surface of the ilium. Am J Phys Anthropol 128:324–339.
İşçan MY, Loth SR. 1986. Determination of age from the sternal rib in white females: a test of the phase method. J Forensic Sci 31:990–999.
İşçan MY, Loth SR, Wright R. 1984a. Age estimation from the rib by phase analysis: white males. J Forensic Sci 29:1094–1104.
İşçan MY, Loth SR, Wright R. 1984b. Metamorphosis at the sternal rib: a new method to estimate age at death in males. Am J Phys Anthropol 65:147–156.
İşçan MY, Loth SR, Wright R. 1985. Age estimation from the rib by phase analysis: white females. J Forensic Sci 30:853–863.
Jackes M. 2000. Building the bases for paleodemographic analysis: adult age determination. In: Katzenberg MA, Saunders SR, editors. Biological anthropology of the human skeleton. New York: Wiley-Liss. p 417–466.
Johnson PA. 1996. A test of the normality assumption in the ordered probit model. Vassar College Working Paper No. 34. Available at http://irving.vassar.edu/faculty/pj/ordprobnorm-test.pdf.
Kemkes-Grottenthaler A. 2002. Aging through the ages: historical perspectives on age indicator methods. In: Hoppa RD, Vaupel J, editors. Paleodemography: age distributions from skeletal samples. Cambridge: Cambridge University Press. p 48–72.
Kimmerle EH, Jantz RL, Konigsberg LW, Baraybar JP. 2008a. Estimation and identification in American and East European populations. J Forensic Sci 53:524–532.
Kimmerle EH, Konigsberg LW, Jantz RL, Baraybar JP. 2008b. Analysis of age-at-death estimation through the use of pubic symphyseal data. J Forensic Sci 53:558–568.
Kimmerle EH, Prince DA, Berg GE. 2008c. Inter-observer variation in methodologies involving the pubic symphysis, sternal ribs, and teeth. J Forensic Sci 53:594–600.
Konigsberg LW, Herrmann NP, Wescott DJ, Kimmerle EH. 2008. Estimation and evidence in forensic anthropology: age-at-death. J Forensic Sci 53:541–557.
Kunos C, Simpson S, Russell K, Hershkovitz I. 1999. First rib metamorphosis: its possible utility for human age-at-death estimation. Am J Phys Anthropol 110:303–323.
Kurki H. 2005. Use of the first rib for adult age estimation: a test of one method. Int J Osteoarchaeol 15:342–350.
Lovejoy CO, Meindl R, Pryzbeck T, Mensforth R. 1985. Chronological metamorphosis of the auricular surface of the ilium: a new method for the determination of age-at-death. Am J Phys Anthropol 68:15–28.
Martrille L, Ubelaker D, Cattaneo C, Seguret F, Tremblay M, Baccino E. 2007. Comparison of four skeletal methods for the estimation of age-at-death on white and black adults. J Forensic Sci 52:302–307.
Milner GR, Wood JW, Boldsen JL. 2000. Paleodemography. In: Katzenberg AM, Saunders SR, editors. Biological anthropology of the human skeleton. New York: Wiley-Liss. p 467–497.
Mueller HG, Love B, Hoppa RD. 2002. Semiparametric method for estimating paleodemographic profiles from age indicator data. Am J Phys Anthropol 117:1–14.
Paine R, Boldsen JL. 2002. Linking age-at-death distributions and ancient population dynamics: a case study. In: Hoppa RD, Vaupel J, editors. Paleodemography: age distributions from skeletal samples. Cambridge: Cambridge University Press. p 169–180.
Prince DA, Kimmerle EH, Konigsberg LW. 2008. A Bayesian approach to estimate skeletal age-at-death utilizing dental wear. J Forensic Sci 53:588–593.
Prince DA, Konigsberg LW. 2008. New formulae for estimating age-at-death in the Balkans utilizing Lamendin's dental technique and Bayesian analysis. J Forensic Sci 53:578–587.
Russell K, Simpson S, Genovese J, Kinkel M, Meindl R, Lovejoy CO. 1993. Independent test of the fourth rib aging technique. Am J Phys Anthropol 92:53–62.
Schmitt A, Murail P. 2004. Is the first rib a reliable indicator of age-at-death assessment? Test of the method developed by Kunos et al. 1999. Homo 54:207–214.
Walker PL, Johnson JR, Lambert PM. 1988. Age and sex biases in the preservation of human skeletal remains. Am J Phys Anthropol 76:183–188.
Weiss AA. 1997. Specification tests in ordered logit and probit models. Econ Rev 16:361–391.
Wittwer-Backofen U, Buba H. 2002. Age estimation by tooth cementum annulation: perspectives of a new validation study. In: Hoppa RD, Vaupel J, editors. Paleodemography: age distributions from skeletal samples. Cambridge: Cambridge University Press. p 119–129.
Yavuz MF, İşçan MY, Çölŏglu AS. 1998. Age assessment by rib phase analysis in Turks. Forensic Sci Int 98:47–54.
Yoder C, Ubelaker DH, Powell JF. 2001. Examination of variation in sternal rib end morphology relevant to age assessment. J Forensic Sci 46:223–227.